



Zentrum für Technomathematik

Fachbereich 3 – Mathematik und Informatik

NUMERICAL EXPERIMENTS FOR THE APPROPRIATE REPRESENTATIVE VOLUME ELEMENT SIZE SELECTION ON THIN TEXTURIZED METALS UNDER MECHANICAL LOADS

Jonathan Montalvo-Urquizo

Mischa Ungermann

Report 12-04

Berichte aus der Technomathematik

Report 12-04

Dezember 2012

Numerical experiments for the appropriate representative volume element size selection on thin texturized metals under mechanical loads

J. Montalvo-Urquiza^{a,*}, M. Ungermann^a

^a*Zentrum für Technomathematik, Fachbereich 3, Universität Bremen, Germany*

Abstract

The construction of a material description in small scales represents a key issue in multi-scale mechanical problems where a numerical homogenization approach is aimed. The numerical construction of a representative volume element (RVE) for the material must include an adequate description of its geometrical structure and mechanical properties.

On the one hand, the material description through a RVE must be large enough to include as many material properties as possible. On the other hand, the RVE must be as small and simple as possible, to avoid expensive computations in the simulation.

In this work, we analyze an strategy for the selection of the adequate RVE size for elastic problems on thin sheets with strong texture. The selection strategy includes the construction of the geometric descriptor as periodic tessellation of the sheets and the stochastic assignment of stiffness matrices for the different material grains inside the RVE. The procedure is illustrated with an example on steel sheets of type DC01 with thickness $50\mu\text{m}$.

1. The RVE calculation in multiscale problems

Modern simulation of many applied problems requires a methodology to include physical phenomena from more than one scale. This is the case of the mechanical deformation problems considered within the Collaborative Research Center 747 “Micro Cold Forming”.

*Corresponding author

Email address: `montalvo@math.uni-bremen.de` (J. Montalvo-Urquiza)

For problems involving micro-components, not only the phenomena at the component scale (large scale) determine the way a material piece react to given forces, but also the phenomena at the scale of material grains (small scale) play a significant roll in the single reactions of a micro-component.

The connection between the scales in the deformation process is modeled following the theory of mathematical homogenization. In practice, this requires a material description at the small scale to be used in calculations and later summarized and sent to the large scale computations. This description is called Representative Volume Element (RVE) and must include all necessary information about how material looks like and behaves at the small scale. Obviously, only an accurate description of material can lead to a proper method simulating both material scales together. For mechanical problems, the RVE must include the geometrical description for a representative amount of material, together with the local properties at this small scale.

On the one hand, the size of the RVE must be large enough to contain enough material information describing a general piece in the small scale and, on the other hand, the RVE must be small enough to keep computational work affordable. This is the reason why the right selection of the RVE size is an important issue when aiming a two-scale simulation. Finding the right compromise between amount of information and small size is a key question on implementing a two-scale simulation of any kind.

In this work, we consider material pieces made of rolled thin sheets and the way of finding a good RVE size for the small scale. In particular, the material considered here contains strong rolling effects in the form of texture, i.e. crystal orientations of single material grains have preferred directions, [1]. One main difficulty on materials with texture is that, although the crystalline structures have the tendency towards one direction, each grain slightly diverts its own orientation. On the other hand, this diversion cannot be determined a-priori and each piece of material will unavoidably have a different set of grain orientations. This stochastic feature of material has been the issue on the previous works [2] and [3].

After presenting the basic aims of this work, the ideas of an algorithm for the construction of RVE geometries are presented in Section 2. The mechanical problem to be solved on every RVE domain and the strategy to find a correct size for the RVE to be representative without becoming too large are the topics of Section 3. Later, the results of the presented

strategy for geometries constructed out of information for Steel DC01 are shown in Section 4 and finally, Section 5 draws some conclusive remarks on the complete procedure.

2. Construction of periodic geometries

In order to describe the shape of a representative material piece, the RVE geometry must consider periodicity. Being periodic, the RVE can be thought as the basic piece used to construct a complete component in the large scale. For the case of thin sheets, where the RVE thickness will be assumed to be the same thickness as for the sheet, there are only two directions in which the periodicity must be enforced. Figure 1 shows a side view of one periodic RVE geometry and the way it can be used to construct a larger piece in form of multiple RVEs joint together.

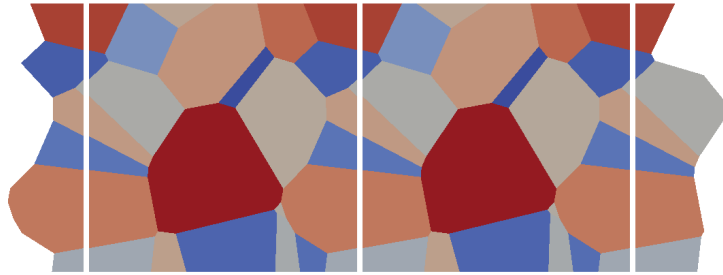


Figure 1: Side view of a periodic sheet of material. The horizontal direction contains periodic grains and multiple copies of a RVE can be used to construct a larger material piece.

One three dimensional example of a RVE geometry with periodicity in the x and y directions is presented in Figure 2. The figure shows the RVE with the constructed subdomains and the tetrahedral mesh constructed for the finite element calculations. Figure 3 shows the six outer faces of the same RVE from Figure 2 where it can be observed how the four faces ordered horizontally contain the periodicity in form of two sets of mirrored domains, while the two faces corresponding to the top and bottom of the RVE present no relation between them.

The RVE geometries presented in this work are assumed to be in the three-dimensional domain $\Omega_{RVE} = [0, s] \times [0, s] \times [0, d]$ with d and s denoting the sheet thickness and the horizontal diameter of the RVE, respectively.

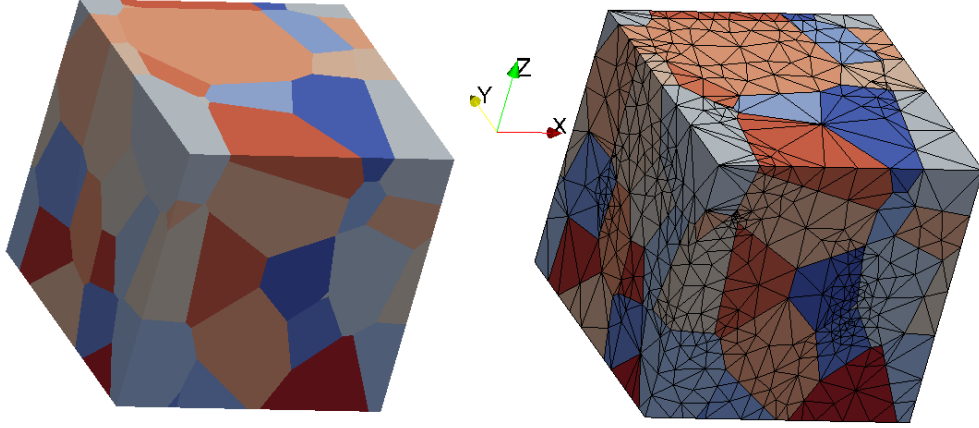


Figure 2: Example of a three dimensional RVE with periodicities in x and y directions. On the right side, the same RVE with the constructed tetrahedral mesh.

The periodic geometries presented here are the result of a computational algorithm including the following steps:

1. Random selection of a set of n points (x_i, y_i, z_i) in Ω_{RVE} to serve as centers of the single grains inside the RVE.
2. Construction of replicas of the grain centers into periodic positions outside the RVE. For the case of two periodic directions this means 8 replicas of each grain center. The replicas belong to the domain $[-s, 2s] \times [-s, 2s] \times [0, d]$ and have the coordinates $(x_i + as, y_i + bs, z_i)$ with $a, b \in \{-1, 0, 1\}$, $(a, b) \neq (0, 0)$.
3. Construction of a domain partition based in a Voronoi tessellation considering all $(1 + 8)n$ centers and replicas together.
4. Extraction of the geometry inside the original RVE domain, keeping track of all regions and their corresponding center index i . This extraction must consider all possible region types present in the partition and intersecting the RVE domain, it is
 - (a) regions fully inside the RVE domain,
 - (b) regions having at least one vertex inside the RVE domain,
 - (c) regions having at least one edge crossing the RVE domain, and
 - (d) regions with a face intersecting the RVE domain.

The geometries presented here are constructed via a C implementation which makes use of some routines of the Qhull package (see [4]) for the tessellation construction and the creation of the necessary region cuts.

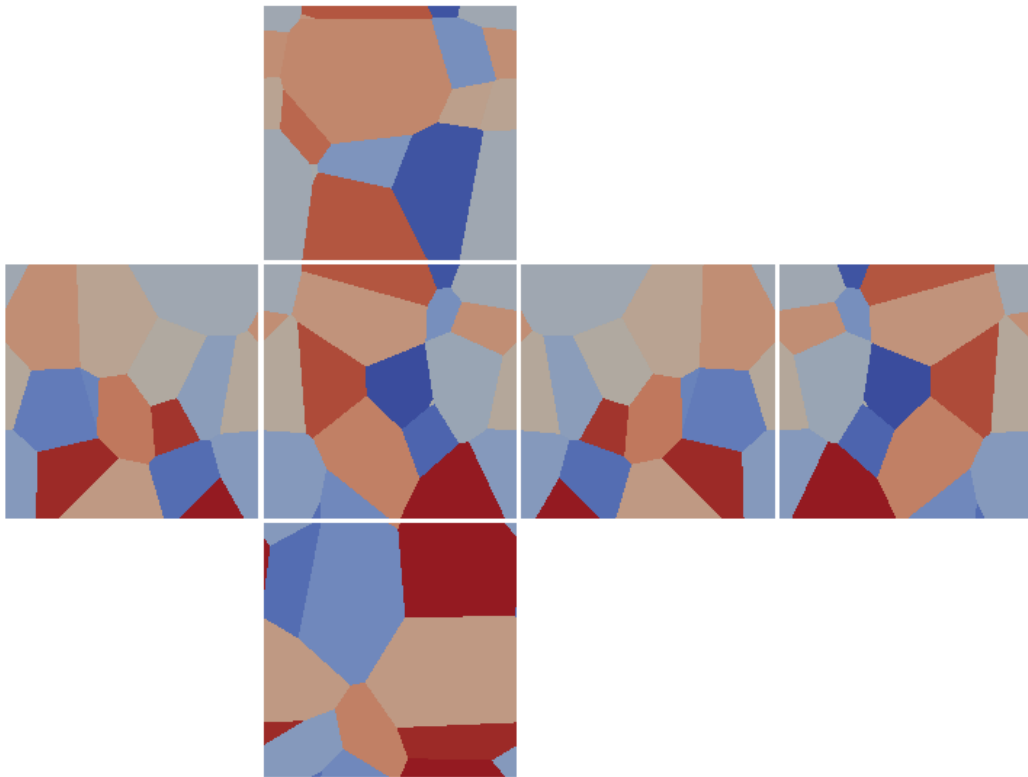


Figure 3: Outer faces of the RVE from Figure 2. The faces are ordered in a constructive form from which one could build the three dimensional RVE boundary by folding along the white borders.

Once a RVE partition has been constructed, the next step is to construct a mesh for finite element computations. The meshing of RVE partitions has been performed with the software TetGen which construct tetrahedral meshes of all regions provided after the four steps above have been performed. For details on the TetGen software see [5] and the references therein.

3. The mechanical problems in RVEs

Following [1] and [2], the local stiffness of each material grain can be modelled using a stochastic model for the texture in the material. The stiffness in the complete RVE can then be described as a function with different values on each partition of the RVE geometry, it is, as a function $C : \mathbb{R}^3 \rightarrow \mathbb{R}^{6 \times 6, sym}$ assigning to the coordinates (x, y, z) a symmetric stiffness $C(x, y, z)$.

The mechanic problem of elasticity for the RVE domain reads

$$-\operatorname{div}(\sigma(x, y, z)) = 0, \quad (1)$$

$$\sigma(x, y, z) = C(x, y, z)\varepsilon(x, y, z), \quad (2)$$

$$\varepsilon(x, y, z) = \frac{1}{2} (\nabla u(x, y, z) + \nabla^T u(x, y, z)), \quad (3)$$

where u , ε and σ denote the deformation, strain and stress, respectively. The boundary conditions are set in accordance with the three different modes of tension and three modes of shear by applying a condition on the displacement at some sides of the RVE geometry. This means that we analyze the material responses on a RVE by solving six mechanical problems as the one in equations (1–3) by fixed values of the stiffness matrix $C(x, y, z)$.

The six elastic problems provide information of the response of the material piece described by the RVE to an applied tension or shear force. The common way to summarize the stress responses and pass them to the larger scale is to compute a volume average over the RVE geometry of every response. This means that for each of the six symmetric components $\sigma_{ij}(x, y, z)$ of the stress tensor $\sigma(x, y, z)$, an integral of the form

$$\bar{\sigma}_{ij} = \frac{1}{V} \int_{\Omega_{RVE}} \sigma_{ij}(x, y, z) dx dy dz \quad (4)$$

must be constructed, where V denotes the volume contained in the RVE geometry. The symmetric tensor

$$\bar{\sigma} = \begin{pmatrix} \bar{\sigma}_{xx} & \bar{\sigma}_{xy} & \bar{\sigma}_{xz} \\ & \bar{\sigma}_{yy} & \bar{\sigma}_{yz} \\ \text{sym} & & \bar{\sigma}_{zz} \end{pmatrix} \quad (5)$$

is the volume averaged response of the RVE to the applied mechanical forces and does not depend on the coordinates (x, y, z) any more. The numerical integrations to obtain the tensor $\bar{\sigma}$ are known as the *homogenization step* in the numerical homogenization literature.

For each of the six tension and shear modes, one can compute an homogenized tensor $\bar{\sigma}$, making altogether a set of 36 elastic responses of the RVE in consideration.

For a well studied material, where enough measurements exist, the additional information must be used to modify the first task in the geometry

construction algorithm from Section 1 where a selection of grain centers is performed. In case measurements about grain sizes and/or distributions is available, this information is used to change from a fully random selection of grain centers, to a distributed selection. The extra information can describe material characteristics like presence of larger grains close to the top and bottom of the material or a preferred direction for the grains to be geometrically elongated.

In this work, we consider Steel sheets of type DC01 and with thickness $50\mu\text{m}$. For these sheets, there are measurements about grain diameters on top, middle and bottom of the material which indicate a larger size (and less occurrence) of grains on top and bottom and a smaller size (and more grains) in the middle vertical section of the sheets. Also, there exist information to fix the amount of grains to 40 grains for a volume of full thickness and an area of $2500\mu\text{m}^2$.

The information about the different grain sizes on top, middle and bottom layers of the DC01 sheets have been used here to design geometries in which the vertical coordinate is constructed by the function

$$z = \begin{cases} d - d(1 - 2\hat{z})^p, & \text{for } \hat{z} \leq 1/2 \\ d + d(2\hat{z} - 1)^p, & \text{for } \hat{z} > 1/2 \end{cases} \quad (6)$$

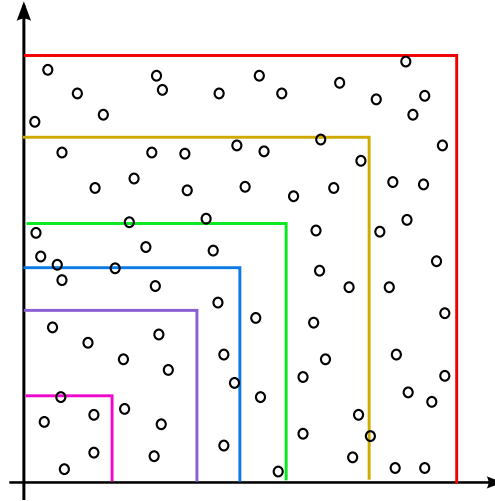


Figure 4: Top view of the schematic arrangement of nested geometries. The grain centers (\circ) from the largest size are the same as from the smaller sizes.

with z in μm and \hat{z} taken as a uniformly distributed variable. This function generates more vertical coordinates in the middle layer of the material for values of $p > 1$. For the results shown here, the measured material grains have been used to set a value of $p = 1.6$ in the generation of vertical coordinates.

To analyze different sizes of RVEs, we consider all samples to have the same thickness as the material and the two horizontal directions will be modified to see how small or large they best fit a numerical simulation. The idea is to calculate the mechanical elasticity problems of tension and shear on a large amount of material samples to obtain statistical distributions of results for different sizes.

In order to compare the different sizes, a large amount of material samples was constructed and pieces of the different sizes were analyzed. Each group of nested pieces was constructed by taking a material geometry of size $s = 100\mu\text{m}$ and then successively taking smaller pieces from it of sizes $s = 80\mu\text{m}$, $s = 60\mu\text{m}$, $s = 50\mu\text{m}$, $s = 40\mu\text{m}$, and $s = 20\mu\text{m}$. The grain centers from the initial piece of size $s = 100\mu\text{m}$ were considered as fixed, making some centers appear in only some or in all pieces, depending on their x and y coordinates. The top view of the nested geometries is illustrated in Figure 4, where the colored lines represent the considered sizes, and the black circles are the fixed centers.

The construction of the geometries for the different RVE sizes consider the included fixed grains inside the corresponding boundary (cf. Figure 4) and the periodic tessellation of this piece with some grains as described in Section 2.

For each size, the included centers were replicated periodically and the process towards the construction of the domain partition and its tetrahedral mesh was performed using the algorithm from Section 2.

4. Simulation results for different RVE sizes

4.1. Example of a nested geometry for Steel DC01

An example is shown in Figure 5 with a set of nested RVEs with the edge lengths $20\mu\text{m}$, $40\mu\text{m}$, $50\mu\text{m}$, $60\mu\text{m}$, $80\mu\text{m}$ and $100\mu\text{m}$. The height of all RVE has been considered as constant and equal to $50\mu\text{m}$. The constant height is equal to the thickness of the steel foil considered and cannot be reduced, as the homogenization theory cannot be applied in this direction.

In Figure 5, it can be seen that the different subdomains, representing the grains in the material, are generated from the same set of centers. However,

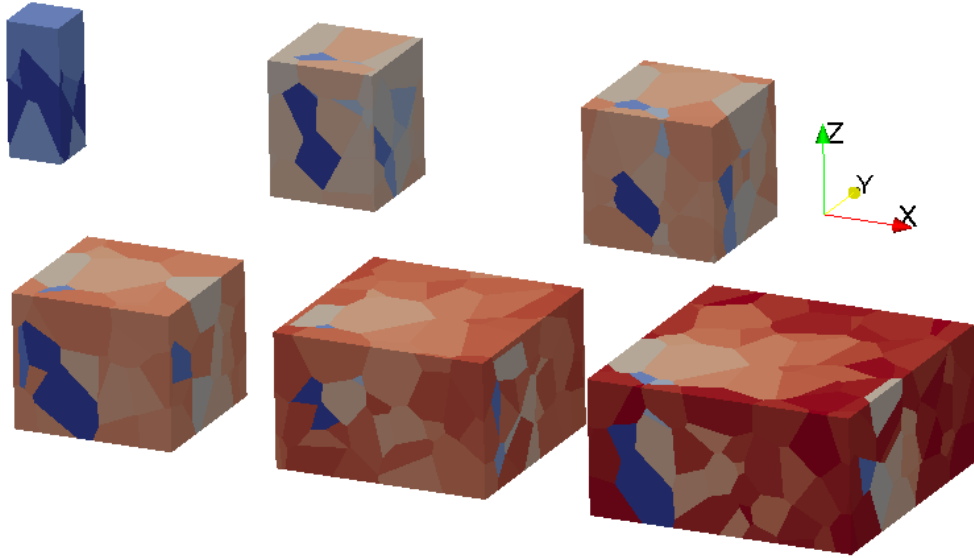


Figure 5: Geometries with subdomains for a set of nested RVEs with edge lengths between $20\mu\text{m}$ and $100\mu\text{m}$. Every subdomain contains the geometrical periodicities in the x and y directions.

the exact configuration of the boundaries differs because of the different conditions for periodicity, having different set of grains to be periodically built in the geometries.

The same geometries have can be tested under elastic loads applied in the three tension and three shear modes. As an example of the results, Figure 6 shows the responses obtained by a unitary strain in the x -direction. It is interesting to note how the grain limits can often be found as large changes in the stress values. The different reactions to applied forces are the result of the assignation of different stiffness for each grain. In this form, the size of the stiffness in the pulling direction is decisive for the size of stress response at each region of the domains.

In fact, the use of analytical and/or numerical homogenization to mechanical problems is based precisely on the idea of certain averaging taking place over large enough material pieces. With respect to Figure 6, the largest and smallest values in the first RVE cannot easily represent the overall material behavior as they are strongly influenced by the specific geometry and stiffness values assigned to it. In contrast to this, for the larger sizes s , the

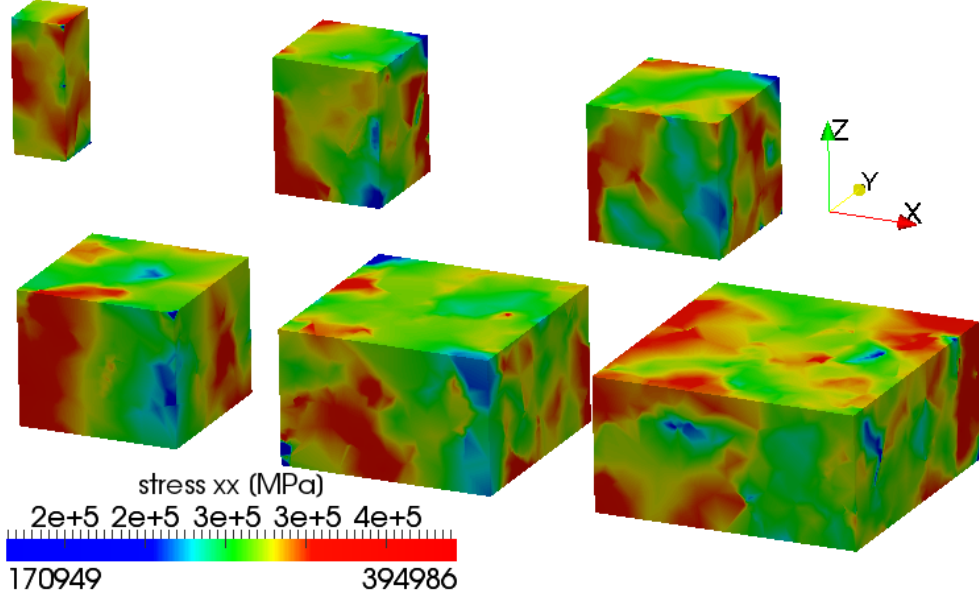


Figure 6: Component xx of the stress responses obtained for a unitary strain in each of the nested geometries shown in Figure 5.

RVEs contain enough large and low values which are *homogenized* and can be expected to deliver a representative average for the material response.

For the nested RVEs in Figure 6, the averaged values of stress as defined in equation (5) are shown in the table below. From this numbers, it can be observed how the tension in the x direction creates large stresses in the yy and zz components as well, while the three shear components remain relatively small for the applied stresses.

s	$\bar{\sigma}_{xx}$	$\bar{\sigma}_{yy}$	$\bar{\sigma}_{zz}$	$\bar{\sigma}_{yz}$	$\bar{\sigma}_{xz}$	$\bar{\sigma}_{xy}$
$20\mu\text{m}$	$+2.993\text{e}+05$	$+8.678\text{e}+04$	$+1.120\text{e}+05$	$-9.981\text{e}+03$	$+1.428\text{e}+03$	$+2.071\text{e}+03$
$40\mu\text{m}$	$+2.998\text{e}+05$	$+8.470\text{e}+04$	$+1.136\text{e}+05$	$-5.800\text{e}+03$	$-2.086\text{e}+03$	$+5.360\text{e}+03$
$50\mu\text{m}$	$+2.986\text{e}+05$	$+8.777\text{e}+04$	$+1.115\text{e}+05$	$-7.770\text{e}+03$	$-4.529\text{e}+02$	$+3.271\text{e}+03$
$60\mu\text{m}$	$+2.991\text{e}+05$	$+8.882\text{e}+04$	$+1.103\text{e}+05$	$-5.883\text{e}+03$	$+1.435\text{e}+03$	$+6.172\text{e}+03$
$80\mu\text{m}$	$+2.990\text{e}+05$	$+8.965\text{e}+04$	$+1.095\text{e}+05$	$-5.823\text{e}+03$	$+7.613\text{e}+02$	$+5.318\text{e}+03$
$100\mu\text{m}$	$+2.995\text{e}+05$	$+9.004\text{e}+04$	$+1.087\text{e}+05$	$-7.482\text{e}+03$	$-6.004\text{e}+02$	$+4.545\text{e}+03$

On the one hand, it is important to consider RVEs with as many information as possible for the material and, on the other hand, there exist a necessity to simplify the computations on single RVEs for an efficient numerical implementation. In practice, finding a good compromise between these two aspects is a key task which can make the difference between an efficient and an impractical multi-scale simulation.

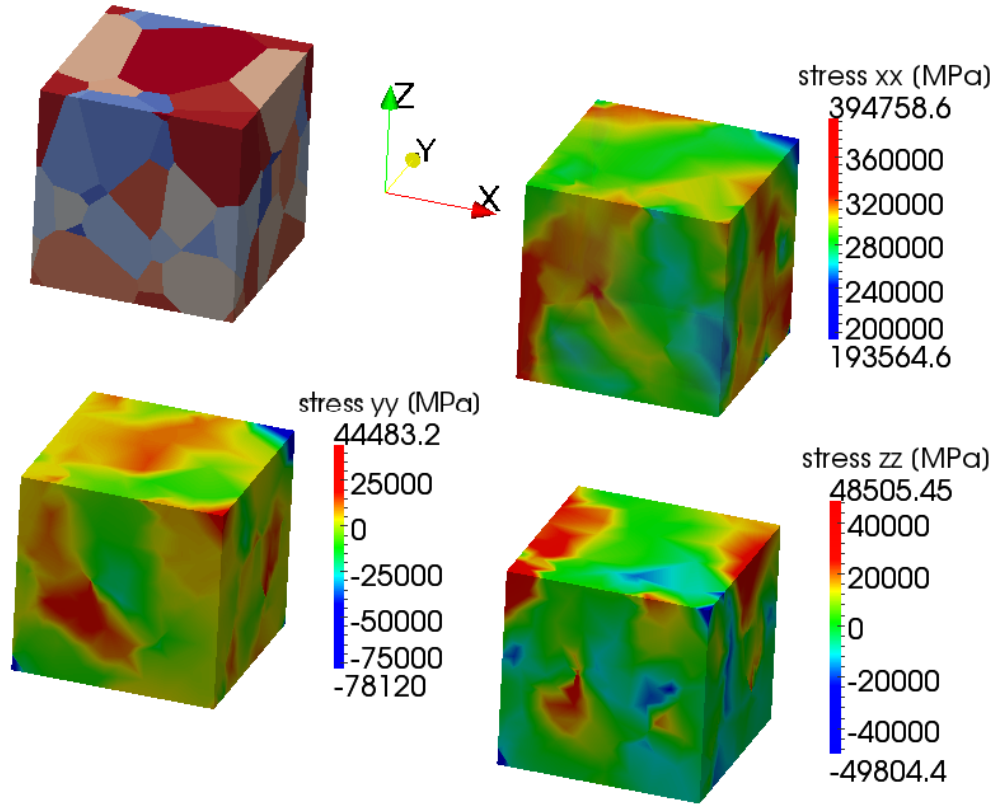


Figure 7: Results of tension in the three directions for a RVE example with edge length $s = 50\mu\text{m}$. The plots show the subdomains defining the grains (top-left), the values of σ_{xx} under a unitary strain in x direction (top-right), the values of σ_{yy} under a unitary strain in y direction (bottom-left), and the values of σ_{zz} under a unitary strain in z direction (bottom-right).

As already mentioned in Section 3, the RVEs can be elastically loaded using six tension and shear modes. Figure 7 considers the $50\mu\text{m}$ RVE from Figure 6 and presents the results for the three tension modes obtained under unitary strain. The colors in the first subplot of Figure 7 show the domain partition through the grains. The colors in the other three subplots correspond to the jj component of stress for a tension of the RVE in the j direction, for $j \in \{x, y, z\}$.

It may be observed how some areas with small stress for the tension in x show large stress for tension in y or z directions. This is a clear results of the single orientations at grain level, producing large stress values by loading

in one direction and low stress values for loading in a different one. The same effect can be observed for other regions with large stress due to tension in y or z .

4.2. Distributions for different RVE sizes

Once it is clear how a realization of nested RVE we are interested in the stochastic distribution for many of such realizations. For this, a large set of M nested realizations have been created and analyzed under action of every elastic mode.

If we only consider the responses of the nested realization while applying a tension mode, we obtain in each realization the responses for every component of $\bar{\sigma}$, making a total of $6M$ responses which can be used to determine the distribution of responses. Altogether, we are able to determine a distribution of every reaction of the different RVEs under each tension and shear modulus, making a total of $36M$ responses.

Figure 8 shows the distributions obtained after applying a unitary tension in x -direction. The subplots in this figure show the different responses (components of $\bar{\sigma}$) expressed as boxplots, marking the median, the 25th and 75th percentiles and the most extreme data points not considered outliers.

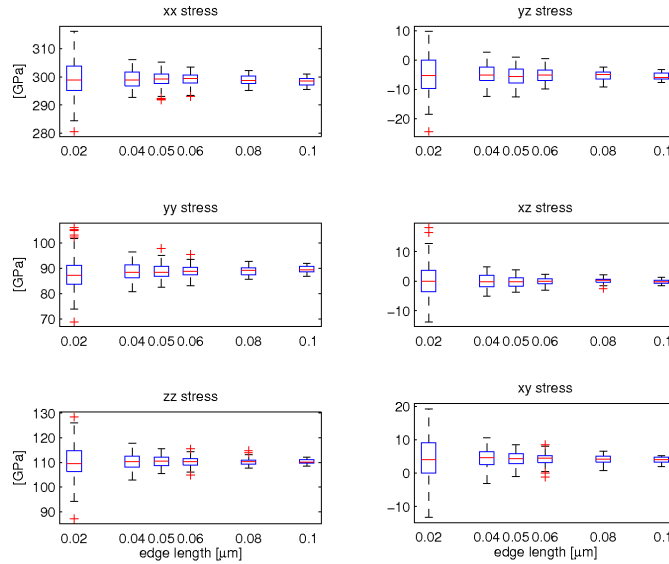


Figure 8: Results for stress components by applying a unitary strain in x direction to a large set of realizations nested in stresses for tension in x direction

To motivate the use of this statistical description, the sets of results for each edge length were subjected to a Jarque-Bera test, a Lilliefors test and a Chi-square test for the null hypothesis, that the underlying data follows a normal distribution. In this example of x tension, only for the stresses in the xz and xy planes of the smallest RVEs two of three tests rejected this null-hypothesis at a 5% significance level.

It is interesting to notice how the distributions show a kind of convergence as the edge lengths s for the RVE become larger. The mean values appear to be kept, while the spread around them continuously decreases as the samples increase their size. A similar effect can be observed for the shear modes. This is illustrated here by Figure 9 where the strain applied was a unitary shear in the yz -plane.

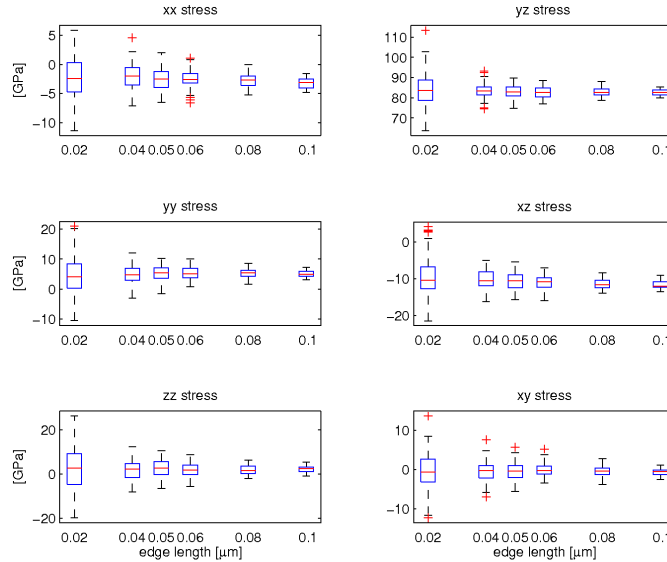


Figure 9: Resulting stresses for shear in yz plane

As already mentioned, there exist six modes and they can all be computed and summarized. This summary is presented in 10 where the box diagrams in each subplot represent the distributions of mean values obtained with the different sizes of RVEs considered. The box diagrams are ordered from bottom to top: $20\mu\text{m}$, $40\mu\text{m}$, $50\mu\text{m}$, $60\mu\text{m}$, $80\mu\text{m}$, $100\mu\text{m}$ in all subplots. The distributions from Figures 8 and fig:yzshear correspond to the first and fourth column of subplots in the summary of results.

The computational effort used to solve the different problems is shown

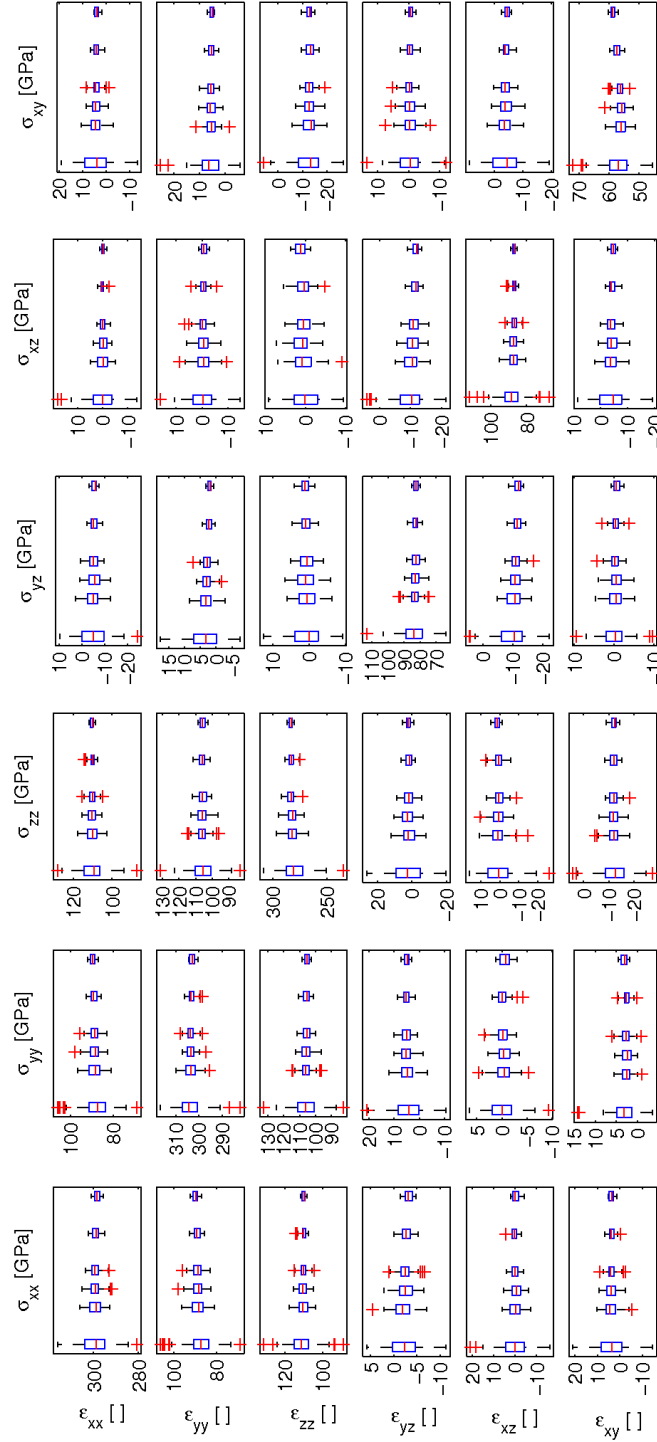


Figure 10: Obtained components of stress (subplots' rows) for all elastic modes (subplots' columns) for different RVE sizes.

in the following table, from where is easy to see how the increase in size is directly reflected in more computational time.

edge length [μm]	# subdomains	average time [s]
20	5	12.1414
40	25	24.4405
50	40	40.9250
60	52	65.4595
80	102	132.5085
100	160	263.8000

The search we intended for can now be easily done by determining how small must be the spread in the distributions from Figure 10. There, it can be observed how the mean values remain constant for the different sizes s of the RVEs while the spread of each distribution decreases for increasing s . As the computational effort strongly increases by making s larger, the size s can now be selected by finding the size s giving a spread smaller than some tolerance (meaning enough material information is inside the RVE) and producing affordable computational times. The question on the affordable computational time depends on the particular multi-scale method to be used and ensures that the evaluations at a larger scale are not so expensive while calling for the responses in the small scale for an RVE.

For example, if we are only interested on having RVEs that can be produced in less than 120 seconds and produce not more than 10 GPa spread for any applied unitary strain, the size $s = 40\mu\text{m}$ would be the best choice, as it already fulfills the spread condition and takes only 40.9250 seconds to be computed.

5. Conclusions

We have shown an algorithm that can efficiently help on the selection of the RVE size for texturized thin metal sheets.

The geometry construction of Section 2 is particularly designed to use a texture model and create computational domains for thin rolled metallic sheets. However, the ideas of periodicity can be easily generalized for any 3D problem with multiple scales.

The modal consideration for the material responses constitutes an effective form of analyzing the spreading of different stress components in dependence of the RVE size and can be used for the best selection together with

the computational times used to obtain results in each RVE size, as described in the last part of the previous section.

It is important to remark that this strategy can be used for a large variety of material. The only necessary ingredients are the knowledge of geometric properties of the grains (cf. Section 2) and a calibrated texture model (cf. [2]) that delivers stiffness tensors for the single material grains. The importance of a calibrated texture model is on the precise mechanical properties for single material grains, being specially important when the rolling process to produce the material has been performed until the thickness d is very small, as in the case of metal foils used in the production of micro components.

Once the optimal choice of the RVE size s has been done, this size can be used to construct a Material Library (cf. [6]) and even to analyze the spreading of stresses on an elasto-plastic computation through the decomposition of total strain into elastic and plastic. For example, for an elasto-plastic model including additive decomposition of strain, the spread of stresses can be computed as the stochastic distributions obtained for the elastic strain $\varepsilon_{elastic} = \varepsilon_{total} - \varepsilon_{plastic}$.

Further considerations regarding the plastic modelling of RVE for metallic materials are works in progress.

Acknowledgements

The authors gratefully acknowledge the financial support by the DFG (German Research Foundation) for the subproject B2 “Allocation Based Simulation” within the Collaborative Research Centre SFB 747 “Micro Cold Forming”.

References

- [1] O. Engler, V. Randle, Introduction to texture analysis: macrotexture, microtexture, and orientation mapping, 2nd Edition, CRC Press, 2010.
- [2] J. Montalvo-Urquiza, P. Bobrov, A. Schmidt, W. Wosniok, Elastic responses of texturized microscale materials using fem simulations and stochastic material properties, *Mechanics of Materials* 47 (2012) 1 – 10. doi:10.1016/j.mechmat.2011.11.008.
- [3] J. Montalvo-Urquiza, P. Bobrov, A. Schmidt, W. Wosniok, Mechanic-stochastic model for the simulation of polycrystals, *PAMM* 10 (1) (2010) 279–280. doi:10.1002/pamm.201010132.

- [4] C. Barber, D. Dobkin, H. Huhdanpaa, The quickhull algorithm for convex hulls, *ACM Trans. on Mathematical Software* 22 (4).
- [5] H. Si, *TetGen: A Quality Tetrahedral Mesh Generator and a 3D Delaunay Triangulator*, Version 1.4.3, WIAS Berlin (2011).
- [6] J. Montalvo-Urquizo, Material libraries for texturized thin metal sheets in elastic range, *PAMM* 12 (1) (2012) 235–236. doi:10.1002/pamm.201210108.